Vol 17 No 11, November 2008
1674-1056/2008/17(11)/4318-05

Chinese Physics B

© 2008 Chin. Phys. Soc.
and IOP Publishing Ltd

The effect of doped ions on single-molecule magnets of the Mn_{12}-Ac family*

Zhang Jun-Rong(张俊荣)[a], He Lun-Hua(何伦华)[a], Cao Hui-Bo(曹慧波)[b], Wang Fang-Wei(王芳卫)[a], and Zhang Pan-Lin(张泮霖)[a]†

[a] *State Key Laboratory of Magnetism, Beijing National Laboratory for Condensed Matter Physics, Institute of Physics, Chinese Academy of Sciences, Beijing* 100190, *China*

[b] *Laboratoire Léon Brillouin, CEA-CNRS, CE-Saclay,* 91191 *Gif-sur-Yvette, France*

(Received 21 April 2008; revised manuscript received 24 April 2008)

This paper investigates the single-molecule magnets of pure and Cr/Fe-doped Mn_{12}-Ac. The components of the mixed crystals are identified by AC susceptibility technique. The ground-state spin and anisotropy parameters of doped Mn_{12}-Ac are obtained: (i) Mn_{11}Cr-Ac (S=19/2, D=0.62 K, B=0.0009 K, Δ=63 K), and (ii) Mn_{11}Fe-Ac (S=21/2, D=0.39 K, B=0.001 K, Δ=55 K). The single-ion origin of the magnetic anisotropy is discussed.

Keywords: single-molecule magnets, magnetic anisotropy, macroscopic quantum tunnelling
PACC: 7550X, 7530G, 7540C

1. Introduction

During the past decade, the single-molecule magnets (SMMs) have attracted considerable interests. They exhibit striking quantum properties, such as quantum tunnelling of magnetization[1−4] and quantum phase interference.[5] And SMMs possess potential technological applications in information storage[6] and quantum computing.[7] Inspired by the future prospects, chemists and physicists have devoted a great deal of efforts to synthesize the room-temperature SMMs. The first molecule behaving as SMMs, $[Mn_{12}O_{12}(CH_3COOH)_{16}(H_2O)_4]\cdot 2CH_3COOH\cdot 4H_2O$ (hereafter Mn_{12}-Ac) has kept the record for the blocking temperature (∼3.4 K) until now. Hence, it is becoming increasingly important for a more fundamental understanding of the origin of magnetic anisotropy.

Mn_{12}-Ac, of the SMMs known to date, has been most widely studied so far by a variety of theoretical approaches and experimental technologies. The strong interest is due to the fact that, to the best of our knowledge, it possesses the best structural quality and the largest magnetic anisotropy barrier. At the same time, many studies have also been carried out on the derivatives of Mn_{12}-Ac. As far as we know, there are three types of variations of Mn_{12}-Ac: (i) replacing the acetate groups with other ligands,[8,9] (ii) reducing the manganese ions with electron donors,[10,11] (iii) substituting the manganese ions by other magnetic metal ions.[12,13] Our group has been exploring the growth of doped Mn_{12}-Ac crystals following a modification of the procedure of Lis,[14] which falls into the third category. We synthesized a series of Cr/Fe/V-doped Mn_{12}-Ac derivatives. It provides an opportunity to investigate how the doped metal ions affect the ground-state spin and the magnetic anisotropy of Mn_{12}-Ac. This work focuses on two simple Cr- and Fe-substituted Mn_{12}-Ac derivatives: Mn_{11}Cr-Ac and Mn_{11}Fe-Ac.

In this paper, we study the effect of doped transition-metal ions Cr and Fe on the spin state and magnetic anisotropy in two crystals Mn_{11}Cr-Ac and Mn_{11}Fe-Ac, respectively. The manuscript proceeds as follows. In the next section, the structural information of two doped Mn_{12}-Ac crystals is given. In Section 3, we identify the components of the mixed crystals by the analysis of AC magnetic susceptibility. Section 4 gives the ground-state spin and anisotropy parameters of Mn_{12}-Ac family, by fitting the equilibrated susceptibilities to Van Vleck equation. The possible single-ion origin of magnetic anisotropy of Mn_{12}-Ac family is also discussed therein. A summary is presented in Section 5.

*Project supported by the National Natural Science Foundation of China (Grant Nos 10505029 and 10375088).
†Corresponding author. E-mail: jrzhang@aphy.iphy.ac.cn

2. Structural information

The magnetic core of the Mn_{12}-Ac cluster consists of a central tetrahedron of four Mn^{4+} (S=3/2), surrounded by a nonplanar ring of eight Mn^{3+} (S=2), as schematically displayed in Fig.1. The strong intracluster exchange interactions stabilize a ground state of the collective spin S=10, in which the spins of the four inner Mn^{4+} ions couple antiferromagnetically to those of the eight outer Mn^{3+} ions each other. The S_4 symmetric Mn_{12}-Ac molecule contains three inequivalent manganese ion sites, labelled here as Mn(I), Mn(II) and Mn(III) using Lis' notation.[14] Each manganese ion has a distorted octahedral coordination geometry with the eight sites occupied by eight oxygen atoms contributed by carboxylate ligations or aqua molecules. Mn^{3+} has strong Jahn–Teller distortion,[15] but Mn^{4+} has none. Mn(I)-site ions have near-perfect octahedral environment, while Mn(II)- and Mn(III)-site ions have tetragonal elongation distortions.

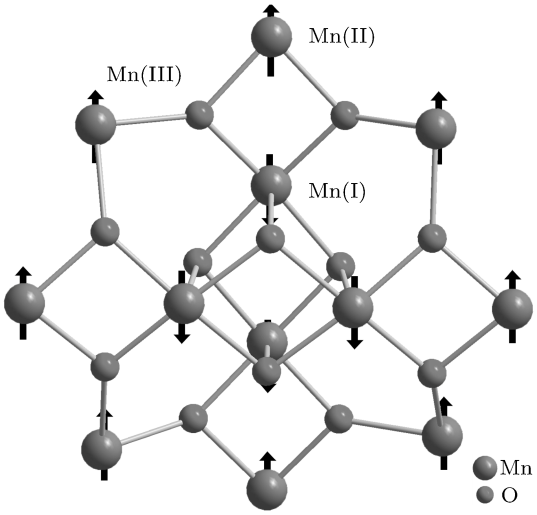


Fig.1. Schematic diagram of Mn_{12}-Ac. Only the magnetic core is plotted.

The single-crystal x-ray diffraction and elastic neutron scattering showed that Cr/Fe doped Mn_{12}-Ac both maintain the crystallographic structure of the parent molecule Mn_{12}-Ac. Furthermore, the extended x-ray absorption fine structure gave the evidence that the doped ions (Cr and Fe) are located at Mn(III) sites in the skeleton of Mn_{12}-Ac.[16,17]

3. Component identification

It is important to point out that the Cr- and Fe-doped Mn_{12}-Ac actually are mixed crystals: Mn_{11}Cr-Ac* and Mn_{11}Fe-Ac*(the star represents mixed crystal). The preparation of the doped Mn_{12}-Ac single crystal is still an open issue. The aim of this section is to clarify the components of the mixed crystals using AC magnetic susceptibility technique.[13]

For single-molecule magnets, the AC magnetic susceptibility is frequency-dependent. Ignoring the high-frequency adiabatic susceptibility,[18] we can write the in-phase and out-of-phase parts of AC susceptibility as follows:

$$\chi'(T) = \chi_0(T)\frac{1}{1+[\omega\tau(T)]^2}, \quad (1)$$

$$\chi''(T) = \chi_0(T)\frac{\omega\tau(T)}{1+[\omega\tau(T)]^2}, \quad (2)$$

where $\chi_0(T)$ is the equilibrated susceptibility, $\omega = 2\pi\nu$ is the angular frequency of the applied AC magnetic field, and $\tau(T)$ is the magnetic relaxation time. According to Eq.(2), the imaginary AC susceptibility $\chi''(T)$ approaches its maximum when $\tau(T) = 1/\omega$. Therefore, there will exhibit different characteristic peaks, corresponding to particular components, in the temperature-dependent curve of χ''.

Figure 2 shows the temperature-dependent curves $\chi''(T)$ of three samples Mn_{12}-Ac, Mn_{11}Cr-Ac* and Mn_{11}Fe-Ac*. The susceptibilities were measured using a Quantum Design PPMS-14T facility. The experimental data were obtained in the 5 Oe (1 Oe≈80A/m) AC magnetic field with a frequency of ν = 33 Hz. In Fig.2(a), there exists one symmetric peak at the temperature of ∼5.5 K for the single crystal Mn_{12}-Ac. Similarly, only one peak is observed for the mixed crystal Mn_{11}Cr-Ac* (see Fig.2(b)). Comparing with Fig.2(a), we find that the position of the peak shifts to the lower temperature and the width is clearly increased. Furthermore, a careful check indicates that the peak is asymmetric and there exhibits a shoulder at ∼4.5 K. The experimental data were well fitted using two Gaussian peaks: one peak at ∼5.5 K and the other at ∼4.7 K. For Mn_{11}Fe-Ac*, it can be seen obviously from Fig.2(c) that there are two peaks at ∼5.5 K and ∼3.2 K, respectively. The peak at ∼5.5 K, observed in all three samples, is naturally attributed to Mn_{12}-Ac. Combining the AC susceptibility analysis of other samples with different doping concentration, the peaks at ∼4.7 K and ∼3.2 K are identified to Mn_{11}Cr-Ac and Mn_{11}Fe-Ac, respectively. Thus the doped Mn_{12}-Ac studied in this work are characterized as two-component crystals: (i) Mn_{12}-Ac/Mn_{11}Cr-Ac (short for Mn_{11}Cr-Ac*), and (ii) Mn_{12}-Ac/Mn_{11}Fe-Ac

(abbreviated as Mn_{11}Fe-Ac*). The doping concentrations were determined by an inductively coupled plasma-atomic emission spectrometry and scanning electron microscope. The molar ratios of Mn_{12}-Ac/Mn_{11}Cr-Ac and Mn_{12}-Ac/Mn_{11}Fe-Ac are 1:1.220 and 1:0.348 in the two samples Mn_{11}Cr-Ac* and Mn_{11}Fe-Ac*, respectively.

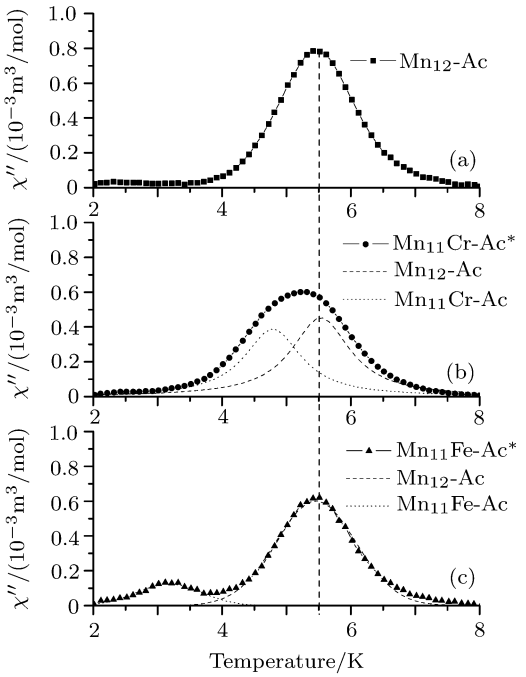


Fig.2. The curves of χ'' vs T: (a) Mn_{12}-Ac; (b) Mn_{11}Cr-Ac*; (c) Mn_{11}Fe-Ac*. The vertical dashed line indicates the position of the characteristic peak of Mn_{12}-Ac. In the figures b and c, the data are fitted using two Gaussian peaks (dashed and dotted for Mn_{12}-Ac and Mn_{11}Cr-Ac/Mn_{11}Fe-Ac, respectively).

4. Results and discussion

The molecular magnets of the Mn_{12}-Ac family can be described by the spin Hamiltonian, to the lowest order,

$$\mathcal{H} = -DS_z^2 - BS_z^4 - g\mu_0\mu_B H \cdot S, \qquad (3)$$

where the first two terms are zero-field splitting (ZFS), D and B are the axial anisotropy parameters, and the last term is the Zeeman energy. The molar equilibrated susceptibility $\chi_0(T)$ in Eqs.(1) and (2) is given by van Vleck equation,[19]

$$\chi_0 = \frac{N_A\mu_0 g^2\mu_B^2}{k_B T} \cdot \frac{\sum_{m=-S}^{S} m^2 \exp(-E_m/(k_B T))}{\sum_{m=-S}^{S} \exp(-E_m/(k_B)T)}, \qquad (4)$$

where N_A is Avogadro constant, k_B is Boltzmann constant. E_m is the energy of the mth of the $(2S+1)$ ZFS energy levels. In the case of the mixed crystal, the in-phase part of ac susceptibility could be phenomenologically expressed as the sum of two-component contributions. In the case of the mixed crystal, the in-phase part of AC susceptibility could be phenomenologically expressed as the sum of two-component contributions. Then we fitted the experimental data of AC magnetic susceptibilities between 8 and 25 K. The choice of the temperature range is based on the following considerations: (i) the quantum tunnelling effect can not be ignored in the temperature below ∼6 K at the experimental frequency of 33 Hz; (ii) the single spin model with S=10 will break down above ∼30 K due to the presence of the excited states.

The in-phase part of ac susceptibilities (symbols and lines for experimental and fitted data, respectively) in the temperature range from 2 to 30 K are plotted in Fig.3. The molar susceptibility is reduced for two doped crystals. It is because of lower spin and smaller energy-level differences for Mn_{11}Cr-Ac and Mn_{11}Fe-Ac, respectively. We reproduced the real AC susceptibilities between 6 and 30 K very well for three samples Mn_{12}-Ac, Mn_{11}Cr-Ac*, and Mn_{11}Fe-Ac*. The deviations from the experimental

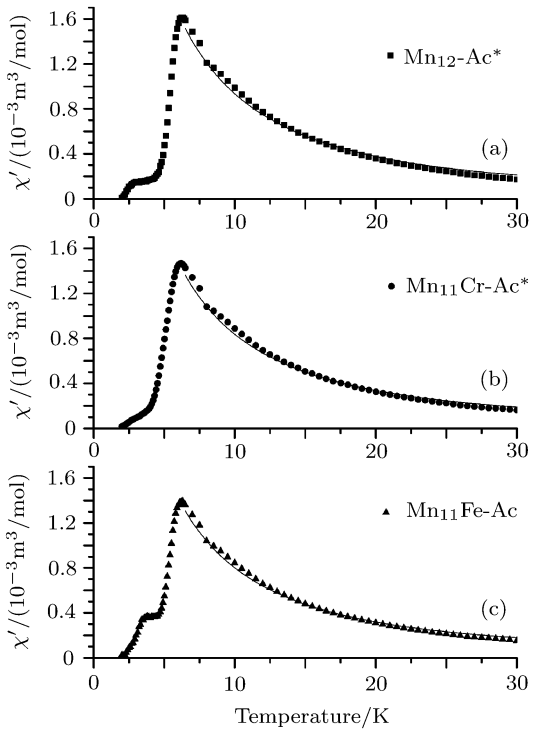


Fig.3. The experimental and fitting curves of χ' vs. T: (a) Mn_{12}-Ac; (b) Mn_{11}Cr-Ac*; (c) Mn_{11}Fe-Ac*. The solid lines are fitted results where the equilibrated susceptibilities χ_0 are calculated using van Vleck equation.

data below 6 K are caused by the slow relaxation. It is emphasized that the vague peaks occurring at ∼2.3 K in Figs.3(a) and 3(c) should be ascribed to the fast relaxation process of minor Mn_{12}-Ac.[20,21] And the best fitting results are shown in Table 1.

Table 1. The ground-state spin, anisotropy barrier and parameters of Mn_{12}-Ac, Mn_{11}Cr-Ac, and Mn_{11}Fe-Ac.

	ground-state spin	anisotropy barrier	anisotropy parameters	
	S	Δ/K	D/K	B/K
Mn_{12}-Ac	10	65	0.53(2)	0.001(2)
Mn_{11}Cr-Ac	19/2	63	0.62(2)	0.000(9)
Mn_{11}Fe-Ac	21/2	55	0.39(1)	0.001(0)

The ground-state spin of the single-molecule magnets Mn_{11}Cr-Ac (S=19/2) and Mn_{11}Fe-Ac (S=21/2) is decreased and increased by 1/2, respectively. It can be concluded that both Cr^{3+} ($3t_{2g\uparrow}$, S=3/2) and Fe^{3+} ($3t_{2g\uparrow}2e_{g\uparrow}$, S=5/2) are in their high-spin states in the Cr- and Fe-doped Mn_{12}-Ac. Moreover, the spin of Cr^{3+} (Fe^{3+}) is parallel to those of Mn^{3+}, and antiparallel to those of Mn^{4+}. The spin configurations are depicted in Fig.4. The reason of Ising-type spin arrangements in doped Mn_{12}-Ac is that the superexchange interactions between Mn(I)–Mn(II) pairs are still dominant as in pure Mn_{12}-Ac.[22] And the nature of the magnetic couplings does not change between the doped Cr^{3+} (Fe^{3+}) and the neighbouring manganese ions. As the result, the spin configurations of the ground state are maintained for the doped Mn_{12}-Ac.

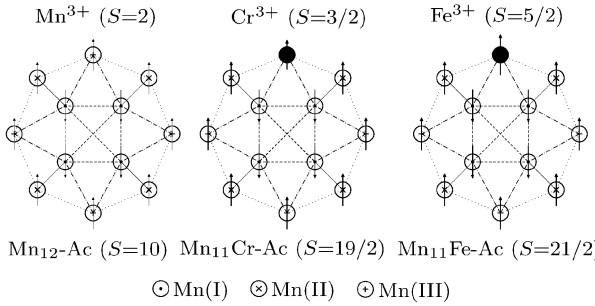


Fig.4. Spin configurations of Mn_{12}-Ac, Mn_{11}Cr-Ac, and Mn_{11}Fe-Ac.

Next, we would like to examine the origin of magnetic anisotropy in Mn_{12}-Ac family and the influence of doped ions on the anisotropy barrier. The anisotropy parameters of Mn_{12}-Ac, obtained by this work, agree with the published results.[23−25] The fit is reliable to the analysis of the magnetic anisotropy. The value of anisotropy parameter D is largely responsible for the anisotropy barrier. The value of anisotropy parameter B is small and of the order of magnitude of 10^{-3} K, but its contribution to anisotropy barrier is non-negligible. From Table 1, it can be seen that the anisotropy parameter D of Mn_{11}Cr-Ac increases remarkably, while decreases for Mn_{11}Fe-Ac. There are two sources for the easy-axis type magnetic anisotropy: single-ion anisotropy and spin–spin interactions. The spin–spin interactions including dipolar and antisymmetric exchange interactions are very weak effects for transition-metal ions. The leading contribution to the magnetic anisotropy of Mn_{12}-Ac comes from the single-ion anisotropy of the strongly Jahn–Teller-distorted Mn^{3+} ions. For the non-Jahn–Teller ions, like Cr^{3+} ($3d^3$) and Fe^{3+} ($3d^5$), the situation becomes very complicated because the orbital degeneracy might be not completely lifted. The single-ion and dipolar contributions are expected to have a comparable magnitude.[26] The large difference in anisotropy parameters of Mn_{11}Cr-Ac and Mn_{11}Fe-Ac may be mainly ascribed to the first-order and second-order spin–orbit couplings.

Now we recall the aim of this work to improve the blocking temperature by doping ions into Mn_{12}-Ac. However, no little progress has been made toward the goal and the heights of anisotropy barrier of the Cr/Fe-doped Mn_{12}-Ac are lower. It is indeed a discouraging result. Clearly there is still a long way to go to understand, predict and control the magnitude of magnetic anisotropy.

5. Conclusions

In this work, the effect of doped ions on structure, spin, and anisotropy are investigated for single-molecule magnets of Mn_{12}-Ac, Mn_{11}Cr-Ac* and Mn_{11}Fe-Ac*. We confirmed that the doped Mn_{12}-Ac still maintains the crystallographic structure of the parent molecule and the doped ion is located at one of Mn(III) sites. The components of the mixed crystals were identified by AC susceptibility measurements. The two doped crystals are characterized as two-component mixed crystals consisting of pure and one-ion substituted Mn_{12}-Ac. The ground-state spin configurations, anisotropy barrier and parameters

were obtained for three types of Mn_{12}-Ac family crystals. The doped ion is in its high-spin state and its spin is parallel to those of the other Mn(III)-site ions. The doping of Cr^{3+} increases the anisotropy parameter D, but reverse for Fe^{3+}. It provides some clues to synthesize the single-molecule magnets with high anisotropy barrier that the single-ion anisotropy should be paid more attention, besides the large spin.

References

[1] Friedman J R, Sarachik M P, Tejada J and Ziolo R 1996 *Phys. Rev. Lett.* **76** 3830

[2] Thomas L, Lionti F, Ballou R, Gatteschi D, Sessoli R and Barbara B 1996 *Nature* (London) **383** 145

[3] Kou S P, Liang J Q, Zhang Y B, Wang X B and Pu F C 1999 *Phys. Rev.* B **59** 6309

[4] Zhang Y B, Liang J Q, Müller-Kirsten H J W, Kou S P, Wang X B and Pu F C 1999 *Phys. Rev.* B **60** 12886

[5] Wernsdorfer W and Sessoli R 1999 *Science* 284 133

[6] Gatteschi D, Caneschi A, Pardi L and Sessoli R 1994 *Science* **265** 1054

[7] Leuenberger M N and Loss D 2001 *Science* **410** 789

[8] Boskovic C, Pink M, Huffman J C, Hendrickson D N and Christou G 2001 *J. Am. Chem. Soc.* **123** 9914

[9] Forment-Aliaga A, Coronado E, Feliz M, Gaita-Arino A, Llusar R and Romero F M 2003 *Inorg. Chem.* **42** 8019

[10] Eppley H J, Tsai H L, de Vries N, Folting K, Christou G and Hendrickson D N 1995 *J. Am. Chem. Soc.* **117** 301

[11] Soler M, Wernsdorfer W, Abboud K A, Huffman J C, Davidson E R, Hendrickson D N and Christou G 2003 *J. Am. Chem. Soc.* **125** 3576

[12] He L H, Yan Q W and Wang F W 2005 *Appl. Phys. Lett.* **86** 202509

[13] Cao H B, He L H, Zhang J R, Zhang X X, Wang F W and Yan Q W 2005 *Phys. Rev.* B **72** 054445

[14] Lis T 1980 *Acta Cryst.* **36** 2042

[15] Jahn H and Teller E 1937 *Proc. Roy. Soc. London* Series A **161** 220

[16] Hachisuka H, Awaga K, Yokoyama T, Kubo T, Goto T and Nojiri H 2004 *Phys. Rev.* B **70** 104427

[17] Cao H B, Chen D F, He L H, Zhang J R, Wang F W, Wu Z Y and Yan Q W 2007 *Chin. Phys.* **16** 0784

[18] Pohjola T and Schoeller H 2000 *Phys. Rev.* B **62** 15026

[19] van Vleck J H 1978 *Rev. Mod. Phys.* **50** 181

[20] Takeda K and Awaga K 1997 *Phys. Rev.* B **56** 14560

[21] Takeda K, Awaga K and Inabe T 1998 *Phys. Rev.* B **57** R11062

[22] Zhang J R, He L H, Cao H B, Wang F W and Zhang P L 2008 *J. Chem. Phys.* **128** 154711

[23] Hill S, Perenboom J A A J, Dalal N S, Hathaway T, Stalcup T and Brooks J S 1998 *Phys. Rev. Lett.* **80** 2453

[24] Mirebeau I, Hennion M, Casalta H, Andres H, Güdel H U, Irodova A V and Caneschi A 1999 *Phys. Rev. Lett.* **83** 628

[25] Amoretti G, Caciuffo R, Combet J, Murani A and Caneschi A 2000 *Phys. Rev.* B **62** 3022

[26] Abbati G L, Brunel L C, Casalta H, Cornia A, Fabretti A C, Gatteschi D, Hassan A K, Jansen A G M, Maniero A L, Pardi L, Paulsen C and Segre U 2001 *Chem. Eur. J.* **7** 1796